Electronic Supplementary Material (ESI) for Nanoscale.

Supporting Information

Influence of carbon dot synthetic parameters on photophysical and biological properties

Pooria Lesani,*[a,b,c] Zufu Lu,[a,b] Gurvinder Singh,[a,b,c] Maya Mursi,[a] Mohammad Mirkhalaf,[a,b,c] Elizabeth J. New,[c,d] Hala Zreiqat*[a,b,c]

[a] Tissue Engineering & Biomaterials Research Unit, School of Biomedical Engineering, the University of Sydney, NSW, 2006, Australia

[b] ARC Training Centre for Innovative BioEngineering, The University of Sydney, NSW, 2006, Australia

[c] The University of Sydney Nano Institute (Sydney Nano), The University of Sydney, NSW 2006, Australia

[d] School of Chemistry, The University of Sydney, NSW 2006, Australia

Table S1 Surface atomic percentage of CDs from XPS.

sample	%C1s	%N1s	%O1s
<3 kDa	60	20.6	19.4
3-10 kDa	60.58	21.6	17.8
10-30 kDa	60.1	22.9	17.0
30-100 kDa	60.47	22.5	17.0

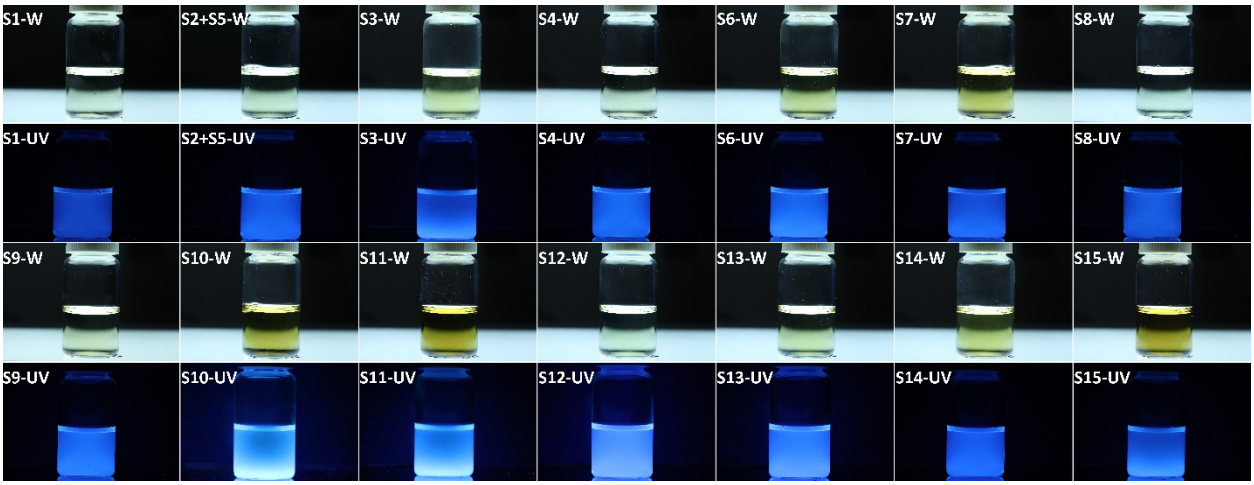

Figure S1 Optical images of all CDs solutions illuminated under white light (W) and 302 nm ultraviolet light (UV): **S1**: E-CD; **S2**: W-CD; **S3**: A-CD; **S4**: 4-CD; **S5**: 8-CD; **S6**: 12-CD; **S7**: 16-CD; **S8**: 0.5-CD; **S9**: 1.0-CD; **S10**: 1.5-CD; **S11**: 2.0-CD; **S12**: <3 kDa-CD; **S13**: 3-10 KDa-CD; **S14**: 10-30 KDa-CD; **S15**: 30-100 KDa-CD.

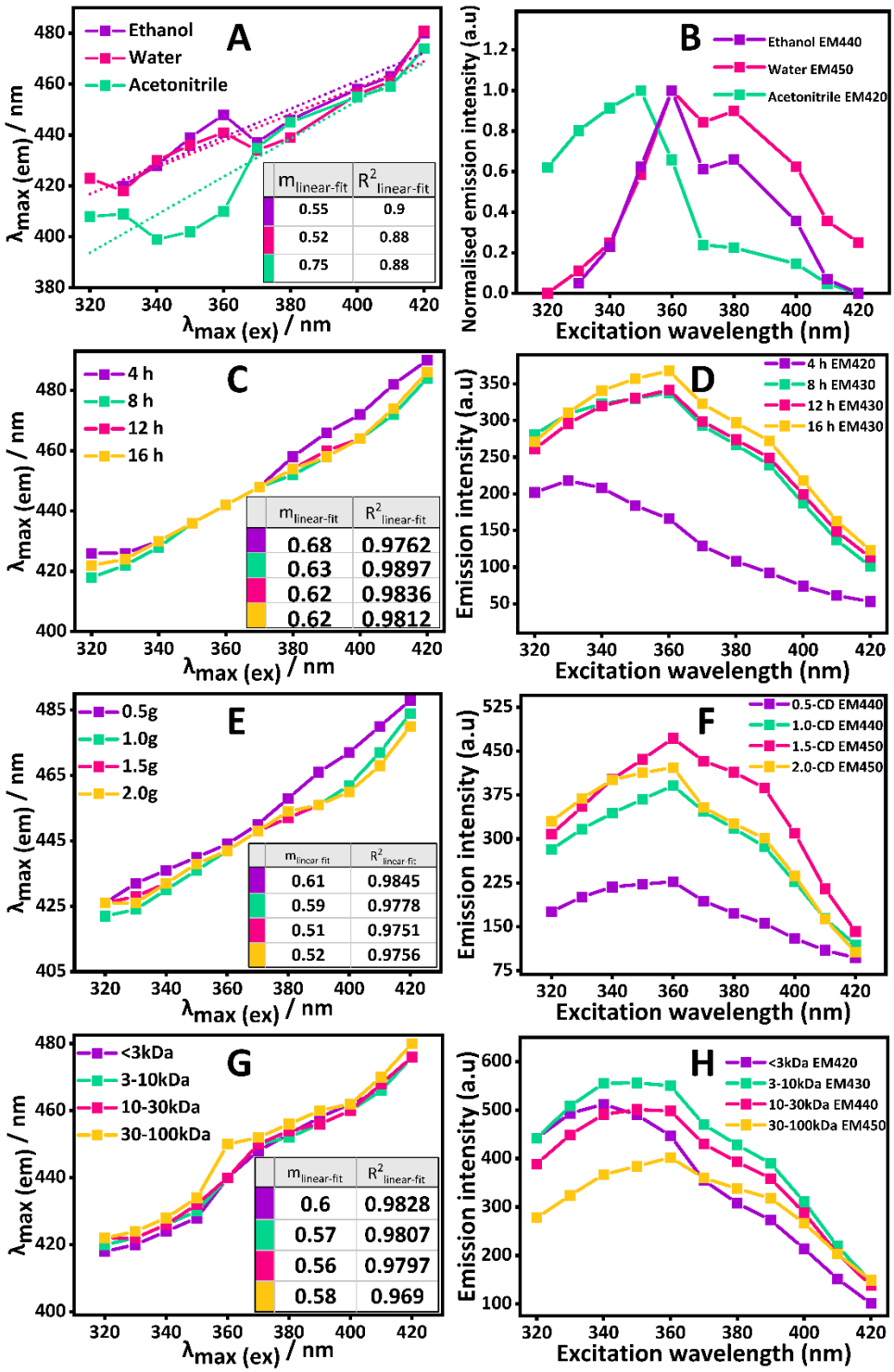

Figure S2 Excitation dependent optical properties of CD synthesized under different conditions, synthesized using different solvent (A-B), different hydrothermal heating time (C-D), different nitrogen dopant quantity (E-F), different particle size distribution (G-H), respectively. (A, C, E, G) peak λ_{em} plotted against λ_{ex} with values for linear fits noted, and (B, D, F, H) emission intensity of emission peaks plotted against λ_{ex} for the different samples at equal concentrations. Regarding abbreviations, $m_{linear\text{-}fit}$ and $R^2_{linear\text{-}fit}$ denote the gradients and coefficients of determination of the linear fits. (C, F, I, L) Plots of integrated PL intensity against absorbance from which QY was calculated for each sample.

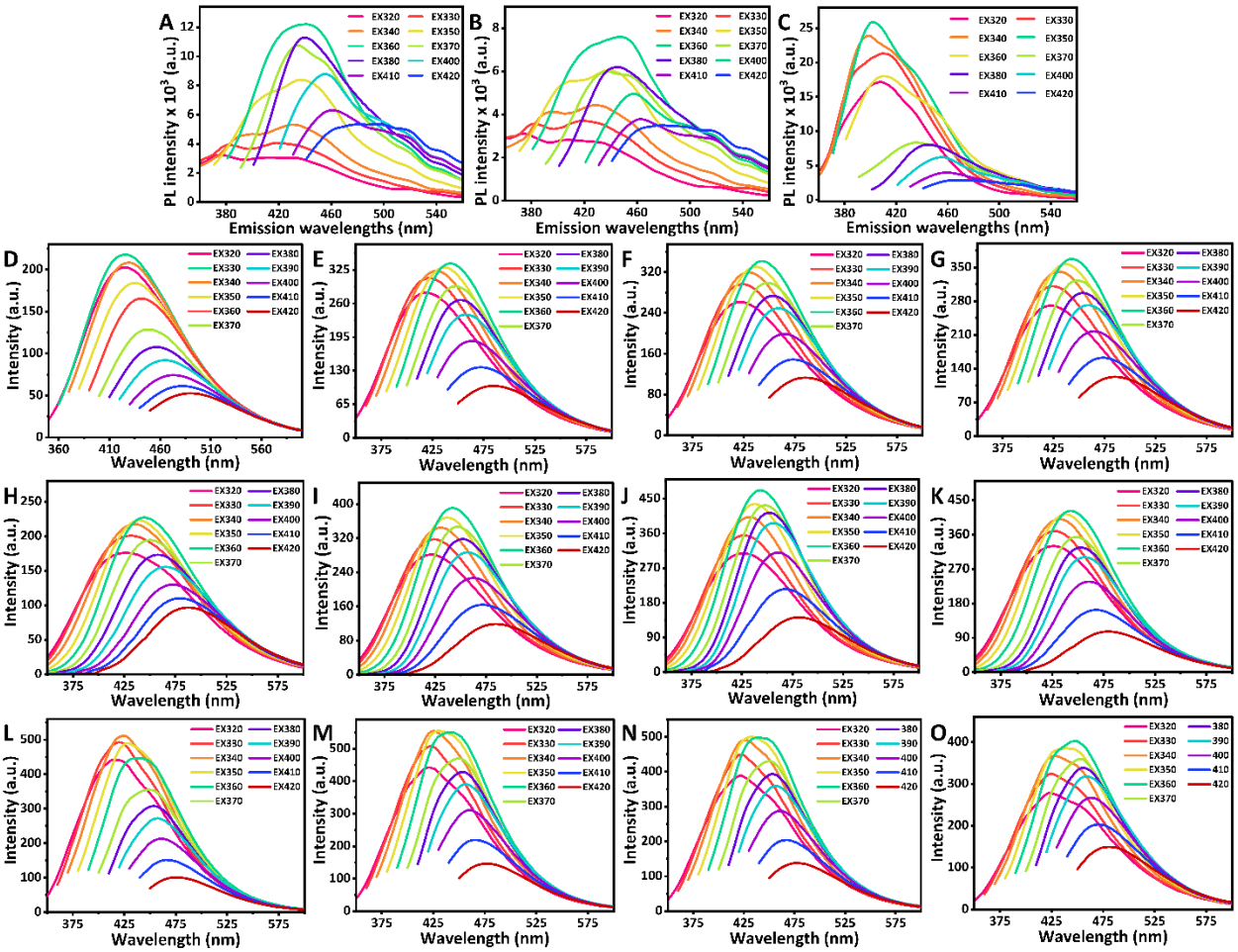

Figure S3 Excitation dependent emissions of CD synthesized under different conditions, synthesized using different solvent (A) Ethanol, (B) Water (C) Acetonitrile; different hydrothermal heating time (D) 4 h, (E) 8 h, (F) 12 h, (G) 16 h; different nitrogen dopant quantity (H) 0.5 g, (I) 1.0, (J) 1.5 g, (K) 2.0 g; different particle size distribution (L) <3 kDa, (M) 3-10 kDa, (N) 10-30 kDa, (O) 30-100 kDa. EX denotes the excitation wavelength.

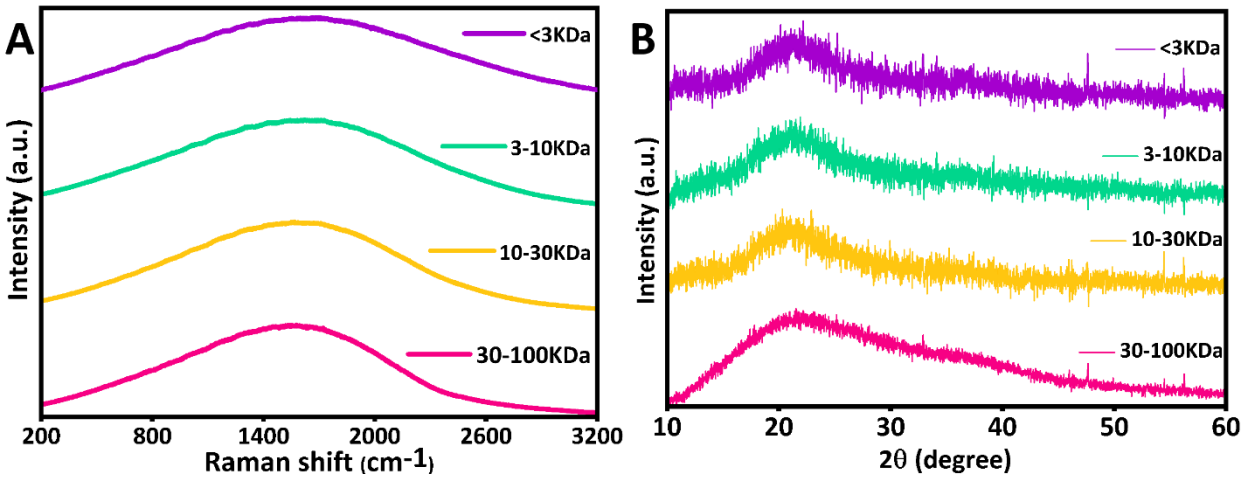

Figure S4. (A) Raman spectra and (B) XRD patterns of CDs with different particle size distribution.

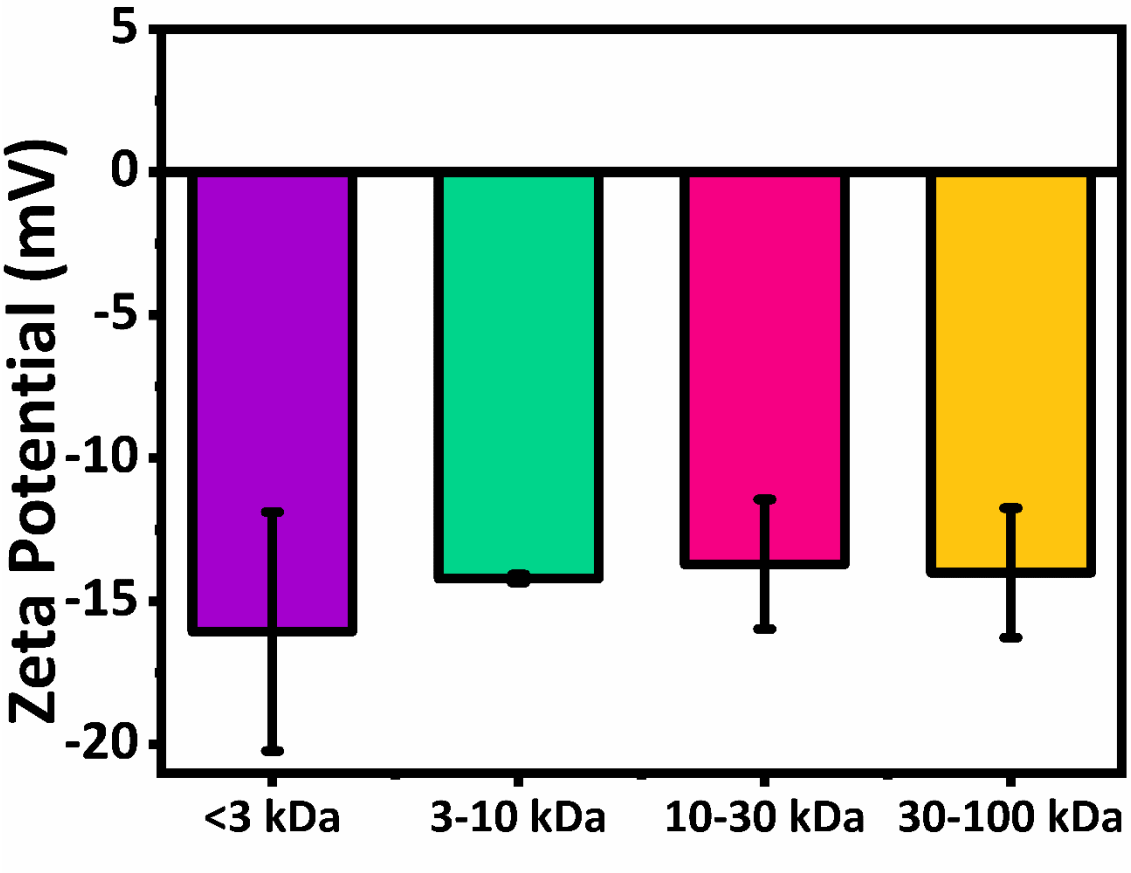

Figure S5 Zeta potential of CD with different particle size distribution.

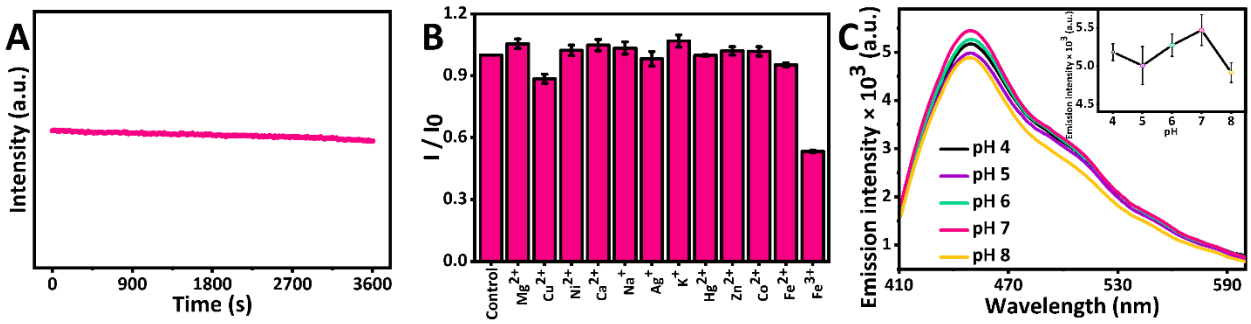

Figure S6 (A) Photostability test of 30-100 KDa-CD under continuous irradiation with UV light (500 W), (B) Specificity of 30-100 KDa-CD to various metal ions at the concentration of 250 µM, (C) Fluorescence emission spectra of 30-100 kDa-CD in HEPES buffer with different pH values (λ_{ex} = 360 nm), inset is pH sensitivity of 30-100 KDa-CD to pH ranging from 4-8 (λ_{em} = 450 nm).

We performed two-photon fluorescence excitation spectroscopy on 30-100 KDa-CD to determine the optimum excitation wavelength. The result showed that the highest emission intensity peak of 30-100 KDa-CD was obtained upon excitation at 750 nm.

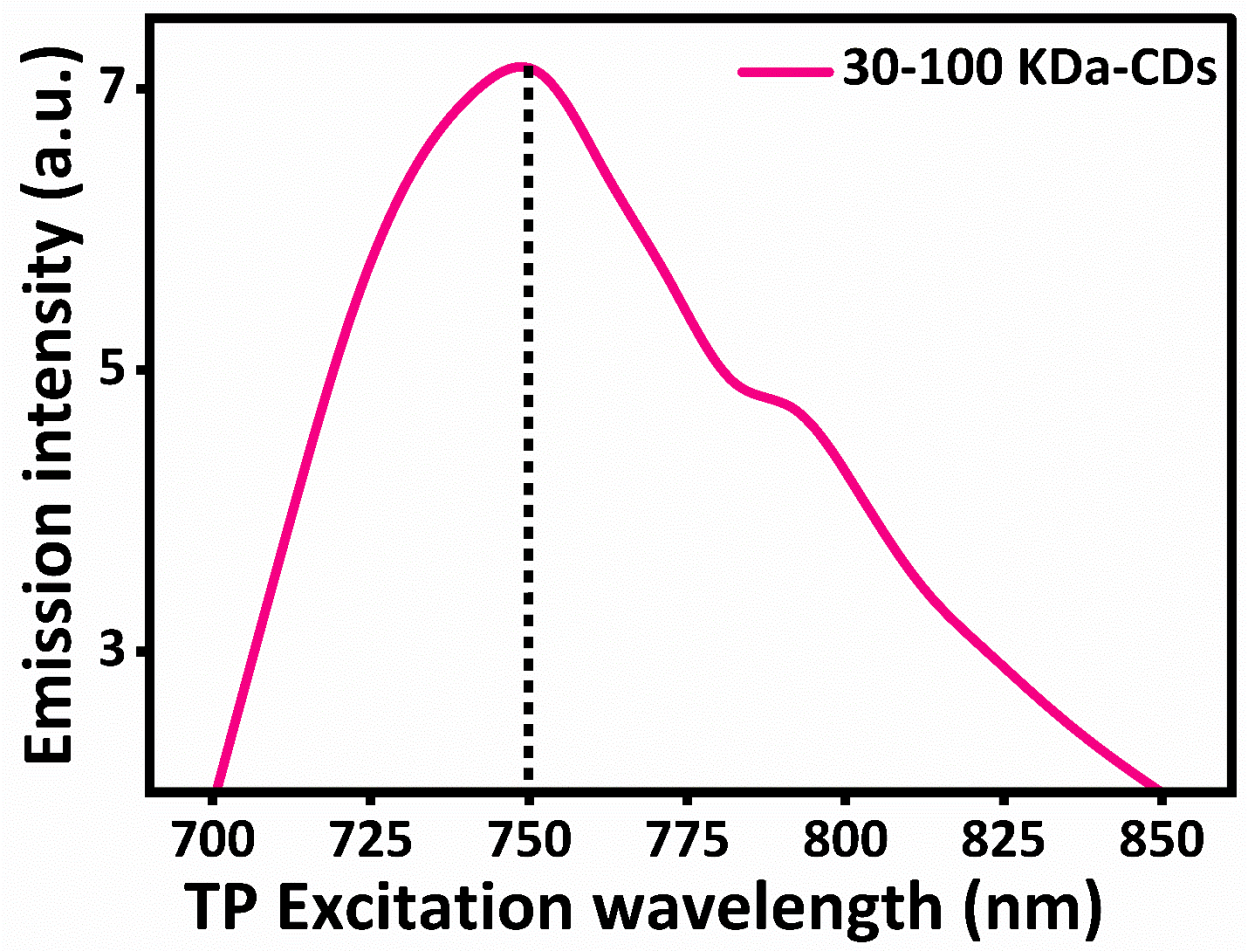

Figure S7 Two-photon fluorescence excitation spectra of 30-100 KDa-CD.